Aerosol Science and Technology 37: 171–182 (2003)

Published by Taylor and Francis
0278-6826/03/$12.00 + .00
DOI: 10.1080/02786820390112678

Cost-Efficiency Analysis of a Model Wire-Plate Electrostatic Precipitator via DNS Based Eulerian Particle Transport Approach

Alfredo Soldati
Centro Interdipartimentale di Fluidodinamica e Idraulica and Dipartimento di Scienze e Tecnologie Chimiche, Università di Udine, Udine, Italy

The object of this work is to outline a methodology that can improve the current procedures used to size cost-optimized, efficient electrostatic precipitators (ESP). Focusing on a model wire-plate ESP initially, we develop a two-dimensional Eulerian, advection-diffusion type model for particle transport with distributed parameters. The Eulerian model is assessed against the accurate Lagrangian particle tracking database obtained for a model ESP using the parameter-free, highly accurate direct numerical simulation database obtained in previous work (Soldati 2000; Soldati and Banerjee 1998). Results show that the simplified Eulerian model can have good performances, provided that the functional form of the required transport parameters (i.e., turbulent dispersion coefficient, electromigration velocity, and convection velocity) are properly defined. Next, the cost function for a model ESP is defined and the influence of several design parameters on cost and collection efficiency is examined to identify guidelines to increase the collection efficiency at the lowest cost. Considering the cost associated with variation of precipitator length and width, wire-to-plate distance, and voltage applied to the wires, results show that the most cost-effective way to increase the collection efficiency of a wire-plate ESP is to decrease the wire-to-wire distance. Furthermore, the reasons for cost effectiveness of wider-spacing ESPs are demonstrated from a theoretical viewpoint, thus confirming the experimental observations of Navarrete et al. (1997).

INTRODUCTION

Electrostatic precipitators (ESPs) are widely used to separate dust particles or aerosols from process or waste gas. Dust particles are charged and driven by an electrostatic field toward the collecting electrodes. Figure 1 shows a schematic representation of the widely used wire-plate configuration.

The collection efficiency of an ESP is influenced by a number of effects such as particle transport, bypass flows, back corona, and particle reentrainment among others (Self et al. 1987). Wire-plate ESPs are characterized by high values of particle collection efficiency for a large range of particle sizes and can be operated with a relatively low pressure drop. The economical downside is represented by the construction or upgrade costs that may be necessary to comply with the new, more stringent regulations on pollution emission. A careful examination of the criteria employed for their design is necessary for effective upgrade or revamping.

The working principle of ESPs is rather simple and yet very difficult to model in detail. Focusing on the most common industrial configuration sketched in Figure 1, the dust-laden gas flows through a rectangular channel bounded by grounded vertical collecting plates; thin vertical wires are placed in the middle of the channel and are maintained at a potential larger than the local electrical breakdown in order to emit ions by corona discharge. The ions charge the initially neutral dust particles entrained by the carrier fluid and interact with the fluid molecules, which acquire momentum and move coherently, generating secondary flows driven by the applied electrostatic field (electrohydrodynamic (EHD) flows). These flows couple the fluid mechanics problem with the electric-field space-charge problem. A further coupling is introduced by the presence of particles that, being charged, are coupled with the electrostatic field and are also coupled with the fluid via the aerodynamic drag (Kallio and Stock 1992; Soldati and Banerjee 1998). To model the effect of all of these phenomena, one should solve the reduced Maxwell equations for the electrostatic field and space charge coupled with both particle dynamics and Navier–Stokes equations. The design and optimization of ESPs depends on the solution of this problem, which can be obtained with a varying degree of accuracy

Received 22 May 2000; accepted 14 August 2002.
The help of Dr. Enrico Monticelli for performing and analyzing model simulations is greatly appreciated. This research was supported by C.N.R. under grant 95.01146.CT03.
Address correspondence to Dr. Alfredo Soldati, Centro Interdipartimentale di Fluidodinamica e Idraulica, Dipartimento di Scienze e Tecnologie Chimiche, Università di Udine, Udine 33100, Italy. E-mail: soldati@uniud.it

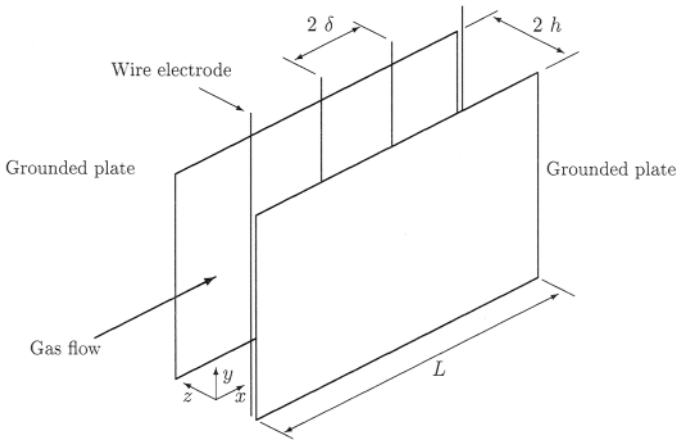

Figure 1. Schematics of wire-plate ESP with the reference coordinate system.

using different models characterized by different degree of complexity and computational cost. We can find different approaches to model particle transport in the fluid, as, for instance, the one-dimensional Deutsch approach (Deutsch 1922), the lumped parameter two-dimensional continuum approach for the fluid and the particulate phase (Eulerian–Eulerian) (Larsen and Sørensen 1984), or the three-dimensional, time-dependent continuum approach for the fluid phase and the Lagrangian approach for the particles (Eulerian–Lagrangian) (Choi and Fletcher 1997, 1998; Soldati et al. 1993, 1997). Current design tools (for instance ESPVI) for particle transport in ESPs are based on the most simplified approaches, which stem from the theory of Deutsch (1922), based on the one-dimensional filter model (Soldati et al. 1997).

In our previous work (Soldati et al. 1993, 1997; Soldati and Banerjee 1998; Soldati 2000) we performed direct numerical simulations (DNS) of the turbulent flow field in plate-plate and wire-plate ESPs and we simulated particle dispersion numerically, including the EHD flows-turbulence coupling using a Eulerian–Lagrangian approach. DNS is a parameter-free method and allows one to calculate the time-dependent, three-dimensional structure of turbulent flows without any modeling of turbulence (Moin and Mahesh 1998). We developed a rather broad database of particle dispersion fields. The database is limited to low Reynolds numbers (about 6,000, based on mean velocity and plate-to-plate spacing) due to the heavy computational requirements. These computational studies have contributed to clarifying the mechanisms of convective transport in ESPs. We observed the influence of the electrostatic field on particle collection efficiency (Soldati et al. 1993, 1997). We observed also that the large-scale structures generated by electrostatic forces modify the turbulence behavior, in particular near the wall, and for certain configurations this might lead to a significant drag reduction (Soldati and Banerjee 1998). Other authors analyzed the performances of industrial precipitators using the Reynolds averaged Navier–Stokes equations (RANS) approach, evaluating the effect of the particle space charge (Choi and Fletcher 1997, 1998) and other electrical processes (Gallimberti 1998) on particle transport. Egli et al. (1997) examined the accuracy of Lagrangian particle tracking into EHD coupled flow fields obtained through a numerical solution of the Euler equation for the gas momentum balance. Other very simple models based on the advection diffusion equation (ADE) have been used to investigate how the precipitator efficiency is influenced by the simultaneous effects of electrical drift, turbulent dispersion, and secondary flows (Larsen and Sørensen 1984) and by the nonuniform electric field (Kihm et al. 1985). ADE has also been used to evaluate the importance of space charge, turbulent dispersion, and particle size distribution on collection efficiency (Ko and Ihm 1997).

If the object is to examine in detail turbulence transport effect, one should use accurate numerics. However, if an optimal configuration is sought, the task of analyzing accurately the influence of a number of different parameters (geometrical dimensions and operative conditions) for a large number of cases can be performed only using models that are sufficiently simple to allow time effective computations. As far as possible, these simple models should account for all of the aspects identified as relevant by more complex investigations.

This article proposes to exploit careful experiments and accurate full-numerical simulations to derive and tune a simpler model that can be used in turn to explore larger ranges of the variables. The final object of our research is to identify possible cost-optimized, high-efficiency configurations for ESPs (Soldati and Marchioli 2001) and to devise a global numerical strategy for ESP optimization and/or control (Beux et al. 2001). Specifically, a distributed-parameter, two-dimensional Eulerian transport model is derived and fitted on DNS data for the calculation of collection efficiency in ESPs. Previous ADE approaches exploit the lumped parameters ADE (Larsen and Sørensen 1984; Kihm et al. 1985; Ko and Ihm 1997; Kim and Lee 1999; Zhuang et al. 2000) fitted on experimental data. In this work, the distributed transport parameters are calculated a posteriori from the DNS data rather than, as usual, from experiments (Williams

and Jackson 1962). The model proposed is accurate and sufficiently simple to be coupled to a cost analysis to examine the influence of design parameters on the final ESP cost.

In this article, we will first present the procedure used to develop the simple two-dimensional Eulerian ADE model, demonstrating its capability to reproduce results obtained with independent experiments (Kihm 1987) and with the time-dependent, three-dimensional DNS (Soldati 2000). Second, we will perform a simple cost analysis of a model wire-plate ESP. The model developed will be used to evaluate particle collection efficiency for changes in the design or operating parameters—wire spacing, plate spacing, wire voltage, and precipitator length—evaluating corresponding costs of the wire-plate ESP.

MODEL FOR PARTICLE TRANSPORT AND ESP EFFICIENCY

DNS Database

DNS is a powerful computational tool to calculate complex turbulent flow fields. DNS is limited by the current computational capabilities to low Reynolds numbers (order of 10,000), yet DNS has the great advantage to be parameter free since it allows one to solve for the three-dimensional, time-dependent turbulence velocity field down to the Kolmogorov scales. In previous work, we analyzed different flow fields for laboratory-scale plate-plate ESP (Soldati et al. 1993) and for wire-plate ESP with different voltages applied to the wires (Soldati and Banerjee 1998). The dispersion of swarms of particles from 4 to 32 μm in these flow fields was then evaluated using a Lagrangian method to track swarms of several thousands of particles. We refer to previous work for detailed accounts (Soldati et al. 1993, 1995, 1997; Soldati and Banerjee 1998; Soldati 2000). Table 1 summarizes the parameters characterizing the available DNS database. The database is used in this work to tune the empirical parameters of a simple transport model and to test its performance. The DNS database comprises simulations made for particles with diameters of 4, 8, 16, and 32 μm subject to one low and one high electrostatic field corresponding to potentials applied to the wire $V = 32$ kV and $V = 42$ kV, respectively. Our objective was to evaluate the effect of particle size and electrical potential on collection efficiency independently of other effects that could complicate analysis and conclusions. Particles were therefore assumed to enter the precipitator precharged. It was also assumed that their charge remains the same along their trajectory, not being a function of the local electrostatic field. This is a realistic assumption since we have chosen a precharge value higher than the maximum charge a particle could acquire when exposed to the ionic space charge of our model ESP. As discussed in Soldati (2000), this approach is the numerical equivalent of the experimental approach adopted in previous work by Kihm (1987) and Self et al. (1987). Our simulation uses a precharge value slightly larger than the maximum charge. Under these assumptions, the charge of a particle is a function of the electrostatic field applied in the precharging section of the ESP via the following equation:

$$q_p = 3\pi \frac{\epsilon}{\epsilon + 2} \epsilon_0 \bar{E}_c d_p^2, \qquad [1]$$

where ϵ_0 is the permittivity of the vacuum, $\bar{E}_c$ is the value of the electrostatic field used for precharging the aerosol particles, and ϵ is the dielectric constant of the particle, which for the present work was equal to 2 (Kihm 1987). In the high intensity case, a uniform precharge field of $\bar{E}_c = 224.7$ kV/m was considered, whereas in the low intensity case it was $\bar{E}_c = 164.8$ kV/m.

Table 1
Summary of DNS database for flow field

Duct width	$2h = 0.04$ m
Duct height	$L_y = 0.1256$ m
Wire-to-wire half spacing	$\delta = 0.0314$ m
Wire length	$l = 0.125$ m
Fluid density	$\rho = 1.29$ Kg/m^2
Fluid kinematic viscosity	$\nu = 1.57 \cdot 10^{-5}$ m^2/s
Reynolds number	$\mathrm{Re} = (U_m\ 2ha)/\nu \approx 6000$
Wire potential	$V = 32$ kV
	$V = 42$ kV

Our database is in good agreement with previous experimental work (Kihm 1987; Kallio and Stock 1992) as discussed in our previous paper. As an example, we will report here a comparison of the overall collection efficiency. An earlier work by Kihm (1987) reported results relative to the collection efficiency of a laboratory scale wire-plate precipitator 5 cm wide. The efficiency of the precipitator, η, is given by the ratio between the number of particles deposited at a given distance from the inlet and the total number of particles at the inlet. Precipitator efficiency for the deposition of 5 μm aerosol droplets with a mean flow velocity of 2 m/s was presented as a function of the Deutsch number, De, that is, the dimensionless streamwise coordinate (Soldati et al. 1995), defined as $\mathrm{De} = (w_e x)/(Ud)$, where x is the streamwise coordinate, d is the duct semiwidth—i.e. the characteristic lateral dimension in a wire-plate precipitator—w_e is the electric migration velocity, and U is the streamwise velocity. Results obtained by Kihm (1987) and those computed from our database for the 4 μm particles in the high potential case are shown in Figure 2. The agreement between computed and experimental data is good.

Two-Dimensional ADE

Predicting the collection efficiency of a precipitator for a large set of values of design parameters using the DNS approach and simulation of particle transport is impossible for current supercomputers. A possible choice for the designer is to rely on the Deutsch equation (1922), which is simple but, reflecting on an over-simplified scenario, leads to large, inaccurate particle deposition rates. A more accurate approach is the use of the particle ADE. Referring to the coordinate system shown in Figure 3, the two-dimensional ADE model may be derived by applying a material balance over the dispersed particles. The

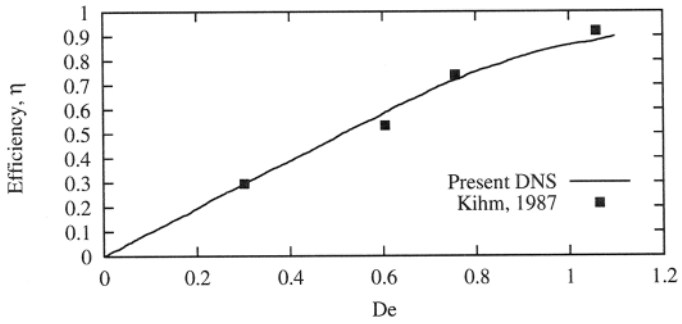

Figure 2. Comparison of results of present DNS to experimental results obtained by Kihm (1987) in similar conditions. Collection efficiency is presented as a function of Deutsch number *De*.

resulting equation is

$$\frac{\partial c}{\partial t} + u_i \frac{\partial c}{\partial x_i} = \frac{\partial}{\partial x_i}\left[D_t \frac{\partial c}{\partial x_i} \right], \qquad [2]$$

where repeated indices imply summation. In Equation (2), u_i are the components of the advection velocity field, D_t is the turbulent dispersion coefficient, and c is particle concentration. In general, all transport parameters—i.e., the advection field and the turbulent dispersion coefficient—are local. However, it may be safely assumed that turbulent dispersion nonuniformities are relevant only in the wall-normal direction. In addition, we observe that turbulent dispersion effects in the streamwise direction are largely overcome by the mean flow advection. Assuming further that the system is in steady state, we may neglect time dependence and obtain the following equation:

$$u(x,z)\frac{\partial c(x,z)}{\partial x} + w(x,z)\frac{\partial c(x,z)}{\partial z} = \frac{\partial D_t(z)}{\partial z}\frac{\partial c(x,z)}{\partial z} + D_t(z)\left[\frac{\partial^2 c(x,z)}{\partial x^2} + \frac{\partial^2 c(x,z)}{\partial z^2} \right], \qquad [3]$$

where $u(x,z)$ and $w(x,z)$ are streamwise and wall-normal particle advection velocities and $D_t(z)$ is the transverse turbulent dispersion coefficient.

To integrate Equation (3), we need to assume a functional form for the flow field parameters $u(x,z)$, $w(x,z)$, and $D_t(z)$. In this work, the detailed knowledge available from our DNS-based Lagrangian tracking database is exploited to derive these functional forms a posteriori. This approach is different from previous work, most of which (Williams and Jackson 1962; Leonard et al. 1980; Larsen and Sørensen 1984) employed lumped-parameter ADE fitted a posteriori on experimental data. In the work by Kihm (1987) there was an attempt to use a "two-region" parameter model for the turbulent dispersion coefficient. Considering that turbulent dispersion must go to zero approaching the wall, Kihm (1987) employed a uniform dispersion value for the central region of the channel and a linear profile for the wall region. However, in our recent works on plate-plate (Soldati et al. 1997) and wire-plate ESPs (Sisti 1997; Monticelli 1999), we found that the use of a uniform or distributed turbulent dispersion coefficient does not reflect on the overall collection efficiency. However, we also found that the model for the

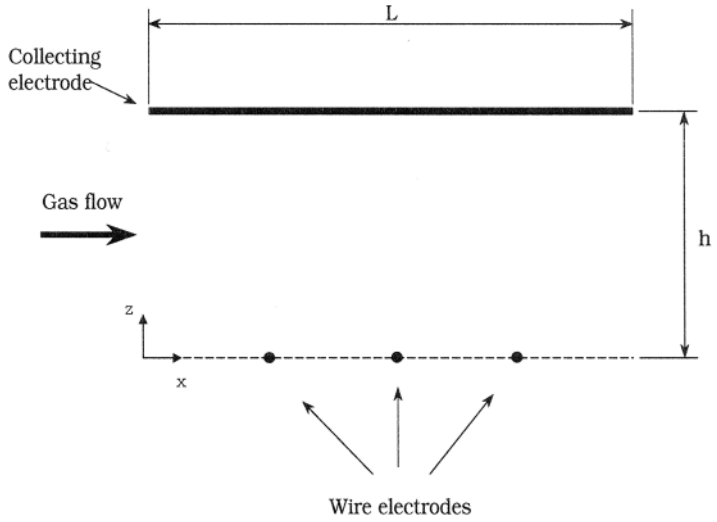

Figure 3. Computational domain for ADE.

advection field has an influence on the particle deposition calculation (Monticelli 1999). We therefore decided to retain the distributed form only for the advection field and to use a uniform value for the turbulent dispersion coefficient. The final form of the ADE we employed is the following:

$$u(x,z)\frac{\partial c(x,z)}{\partial x} + w(x,z)\frac{\partial c(x,z)}{\partial z} = D_t\left[\frac{\partial^2 c(x,z)}{\partial x^2} + \frac{\partial^2 c(x,z)}{\partial z^2}\right]. \quad [4]$$

To solve Equation (4) for $c(x,z)$, it is necessary to assign a functional form for the streamwise advection velocity, $u(x,z)$, and the wall-normal advection velocity, $w(x,z)$, and to give a value for the turbulent dispersion coefficient, D_t. The choice of these transport parameters is described in detail in the next section. Once the transport parameters are fixed, Equation (4) can be integrated with the usual boundary conditions (Larsen and Sørensen 1984; Ko and Ihm 1997). Since the channel centerline is a symmetry line, the resolved computational domain is half the precipitator width (Figure 3). Boundary conditions are fixed as follows: (i) assigned concentration at the inlet section ($x = 0, z = 0 \div h$), (ii) zero flux at the symmetry plane ($x = 0 \div L, z = 0$), (iii) zero gradient in the wall normal direction at the collecting plate ($z = h, x = 0 \div L$), and (iv) zero gradient at the outlet section of the ESP ($x = L, z = 0 \div h$). We used a pseudo-transient approach to find the steady-state solution, starting our calculation from a zero concentration value all over the computational domain. At each time step, the solution is calculated using a line-Gauss Seidel method. The solution converges over time toward the steady-state solution. The steady-state concentration field depends on the dimensions of the domain of integration, L and h, and on the operating conditions for the ESP, which influence the values of the fluid parameters, $u(x,z)$, $w(x,z)$, and D_t. This dependence permits the evaluation of the influence these different parameters have on particle collection efficiency, which is calculated as

$$\eta = \frac{\int_o^h c(0,z)\mathrm{d}z - \int_0^h c(L,z)\mathrm{d}z}{\int_0^h c(0,z)\mathrm{d}z}, \quad [5]$$

where $x = 0$ and $x = L$ are inlet and outlet sections of the ESP, respectively.

Transport Parameters

To solve Equation (4), it is necessary to model advection velocities and turbulent dispersion. The time-averaged advection velocity field may be represented as the superposition of 3 terms: the *streamwise advection field*, strongly related to the mean flow profile, the *wall-normal electrostatic advection field*, directly dependent on the local strength of the electric field, and the *electrohydrodynamic (EHD) advection field*, which accounts for large-scale vortices due to the interaction between fluid molecules and ions generated by corona wind. In our recent work (Soldati 2000), we examined the influence of EHD flows on the local and overall behavior of particles. We found that even though EHD flows have an influence on local particle behavior, in practice this effect averages out when examining the overall particle fluxes. In this analysis, the influence of EHD flows is ignored.

Streamwise Advection Field, u(x, z)*.* Particle streamwise velocity is influenced by the turbulent velocity profile of the fluid and by the electrostatic field. As discussed in Soldati (2000), the effect of the electrostatic field is to modify particle streamwise velocity that is different from fluid streamwise velocity, which in turn is different from that of a duct flow because of the presence of EHD flows. Despite these complex effects, after several tests we considered that a standard logarithmic profile for the mean streamwise particle advection velocity would be sufficiently descriptive for $u(x,z)$ to be used in an ADE equation (Tennekes and Lumley 1976). In contrast, a plug-flow profile, as for instance that applied by Leonard et al. (1980) or by Kihm (1987), leads to a larger inaccuracy.

Wall-Normal Electrostatic Advection Field, w(x, z)*.* If we neglect the EHD flows, the advection velocity field toward the wall is given by the electrostatic migration velocity only. Since we use precharged particles, this parameter accounts for all Coulomb force related effects. In steady state, it is possible to balance electrostatic and drag forces acting on particles, obtaining an expression which, for Stokes drag ($\mathrm{Re}_p \leq 1$), is called Stokes reference velocity, $\mathbf{u}_{st}$. Here, $\mathbf{u}_{st}$ is the velocity of particles relative to the fluid. The streamwise component of $\mathbf{u}_{st}$ accounts for the velocity difference between charged particles and the fluid due to the electrostatic field. The wall normal component of $\mathbf{u}_{st}$ accounts for the electromigration velocity of particles toward the collecting plate. It is known that in wire-plate ESPs, particles are subject to drag forces larger than Stokes drag, so that their actual velocity $\mathbf{u}_{el}$ is lower than $\mathbf{u}_{st}$. Since full a priori evaluation of the wall-normal migration velocity is impossible, in this paper we propose the following expression fitted based on the results of the Lagrangian tracking in DNS flow field:

$$\mathbf{u}_{el}(x,z) = k\mathbf{u}_{st}(x,z) = k\frac{q_p\mathbf{E}(x,z)}{3\pi\mu_f d_p}, \quad [6]$$

or by components,

$$u_{el}(x,z) = ku_{st}(x,z) = k\frac{q_p E_x(x,z)}{3\pi\mu_f d_p},$$

$$w_{el}(x,z) = kw_{st}(x,z) = k\frac{q_p E_z(x,z)}{3\pi\mu_f d_p}.$$

Since the mean fluid velocity is zero in the wall normal direction, $w_{el}(x,z)$ is the term corresponding to $w(x,z)$ in Equation (4). The parameter $k \leq 1$ is a correction coefficient that we derived from DNS data as follows:

$$k = \frac{\int_0^L\int_0^h w_{el}(x,z)\,\mathrm{d}x\,\mathrm{d}z}{\int_0^L\int_0^h w_{st}(x,z)\,\mathrm{d}x\,\mathrm{d}z} = \frac{\overline{w_{el}}}{\overline{w_{st}}}, \quad [7]$$

Table 2
Reference Stokes velocity, actual migration velocity, and coefficient k for different particles in different flow fields and under different applied voltages

d_p	$V\,[kV]$	$\overline{w_{el}}$ [cm/s]	$\overline{w_{st}}$ [cm/s]	k
4 μm	42	6.25	7.54	0.829
	32	3.29	4.18	0.787
8 μm	42	13.62	15.15	0.899
	32	7.02	8.35	0.841
16 μm	42	25.25	30.28	0.837
	32	14.56	16.64	0.875
32 μm	42	40.61	60.57	0.670
	32	25.92	33.41	0.776

where L and h are precipitator length and half-width, $\overline{w_{el}}$ and $\overline{w_{st}}$ are the average wall-normal components of $\mathbf{u}_{el}(x, z)$, which may be obtained directly from DNS data, and of $\mathbf{u}_{st}(x, z)$, which may be obtained from the electrostatic field. The local value of the electrostatic field, $\mathbf{E}(x, z)$, may be calculated solving the reduced set of the Maxwell equations, as is currently done. Procedures may be found in previous work (Leutert and Bohlen 1972; Yamamoto and Velkoff 1981). A summary of the reference Stokes velocity, of the actual migration velocity, and of the k coefficient calculated from our DNS database is presented in Table 2.

Turbulent Dispersion Coefficient. In wire-plate ESPs the turbulent flow field is strongly nonhomogeneous and anisotropic. However, in this work we consider only the effects related to transverse turbulent dispersion, since effects in the streamwise and spanwise directions do not appear as relevant to particle-collection efficiency as those in the transverse direction (Leonard et al. 1980). Transverse turbulent dispersion is related to the intensity of turbulent fluctuations in the z direction, which is almost uniform in the central region of the duct and goes to zero at the wall (Kihm 1987). Similar behavior may be expected from the turbulent dispersion coefficient, which should go to zero in the wall layer. For simplicity, and with the practical application of the results in mind, the theory of diffusion in homogeneous turbulence (Taylor 1921) was used to evaluate the dispersion coefficient in the central, nearly homogeneous region and a uniform value of this coefficient was assumed for the entire width of the duct. Clearly this leads to overestimation of the effects of transverse dispersion on particle transport in the wall layer. Further discussion on this topic may be found in Kontomaris and Hanratty (1994) and in Soldati et al. (1997).

Following Taylor (1921), we calculated the turbulent dispersion coefficient, D_t, from the DNS-based Lagrangian tracking database as the time rate of growth of variance (RGV) for the calculated swarm of particles as follows:

$$D_t = \lim_{t\to\infty} \frac{1}{2}\frac{\mathrm{d}\langle z^2\rangle}{\mathrm{d}t}, \qquad [8]$$

Table 3
Turbulent dispersion coefficient for different particles in different flow fields and under different applied voltages

d_p	$V\,[kV]$	$D_t\,[\frac{m^2}{s}]$
4 μm	42	$7.85 \cdot 10^{-5}$
	32	$9.42 \cdot 10^{-5}$
8 μm	42	$5.66 \cdot 10^{-5}$
	32	$8.06 \cdot 10^{-5}$
16 μm	42	$4.17 \cdot 10^{-5}$
	32	$6.12 \cdot 10^{-5}$
32 μm	42	$2.83 \cdot 10^{-5}$
	32	$3.84 \cdot 10^{-5}$

where $\langle z^2\rangle$ is the variance (mean square displacement, MSD) of the displacement distribution, defined as

$$\langle z(t)^2\rangle = \frac{1}{N(t)}\sum_{n=1}^{N(t)}\left[(z_n(t) - z_n(0)) - \frac{1}{N(t)}\sum_{n=1}^{N(t)}(z_n(t) - z_n(0))\right]^2, \qquad [9]$$

where $N(t)$ is the number of particles in the swarm. Taylor showed also that in the early stages of cloud dispersion, variance increases at a rate proportional to t^2 , whereas after a characteristic time, T_z, usually termed as *integral Lagrangian time-scale*, it relaxes to a linear slope. Calculated D_t for all particle sizes are reported in Table 3.

Testing of Assumptions

To verify the adequacy of the assumptions on transport parameters, we performed a set of numerical tests. The results obtained by the ADE were compared to previous experimental data obtained at Stanford University by Kihm (1987) and to our database (Sisti 1997).

Figure 4 shows the behavior of 4, 8, 16, and 32 μm particles (from top to bottom) in both the high ($V = 42$ kV) and low ($V = 32$ kV) potential case (on the left and on the right part in the figure, respectively). The same figure illustrates the collection efficiency predicted by (i) the lumped parameter—i.e., uniform velocity and uniform turbulent dispersion—ADE method (i.e., of the type used in Williams and Jackson (1962) and Ko and Ihm (1997)), (ii) the present distributed parameter ADE method, and (iii) DNS. From the comparison among collection efficiencies, we observe that the present distributed model is more accurate than the lumped parameter model in comparison to the DNS database, in particular at high values of the collection efficiency. There are deviations between the present ADE and DNS results for 4 μm particles, low potential case (Figure 4b), and for 32 μm particles, high potential case (Figure 4g). In these cases, the present ADE overestimates and underestimates intermediate values of collection efficiencies, respectively. In the high efficiency region, the difference between present ADE- and DNS-based results is smaller, and present ADE gives a more

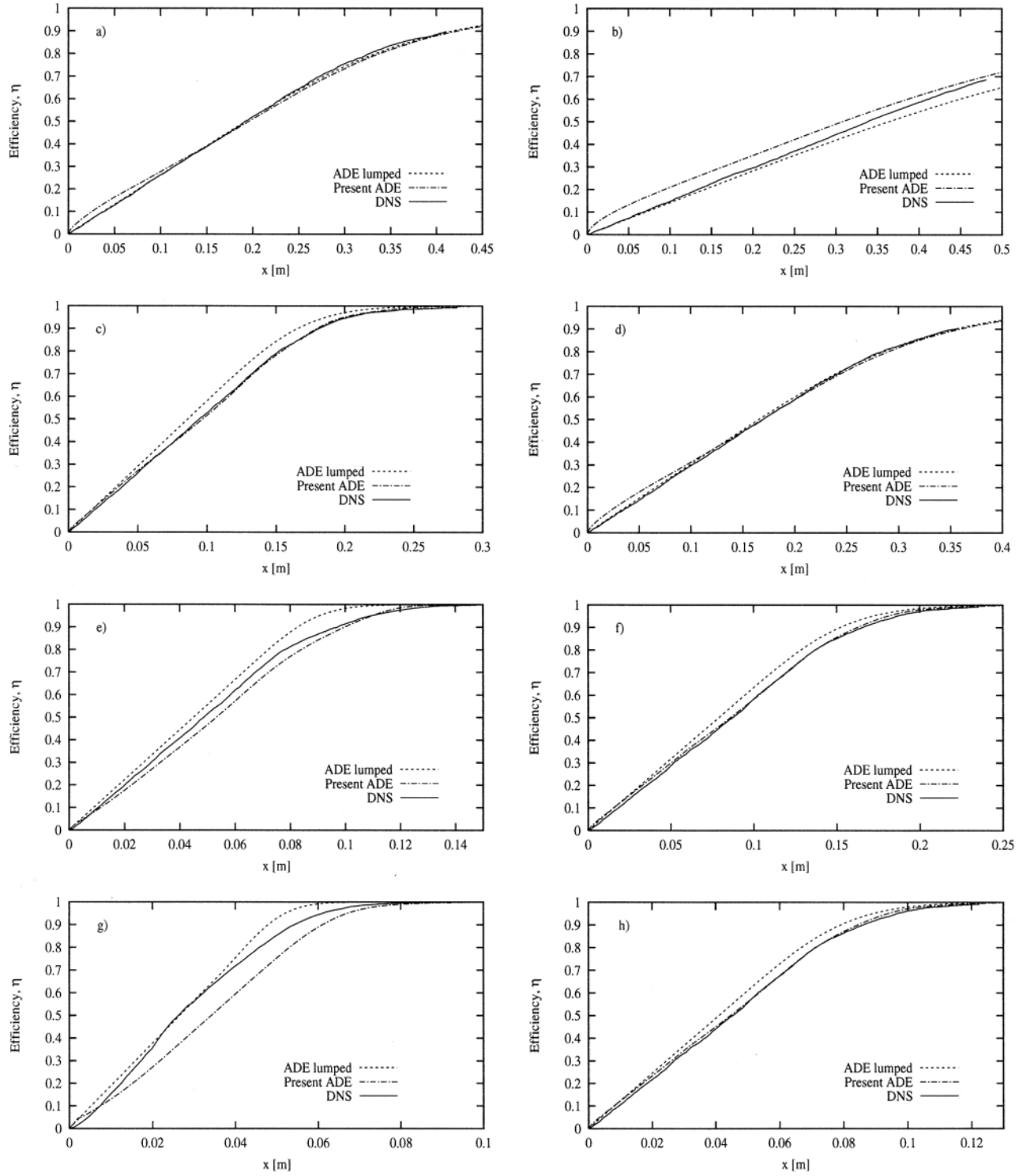

Figure 4. Comparison of prediction of present ADE model to ADE lumped and DNS data for (a) 4 μm particles, high voltage, (b) 4 μm particles, low voltage, (c) 8 μm particles, high voltage, (d) 8 μm particles, low voltage, (e) 16 μm particles, high voltage, (f) 16 μm particles, low voltage, (g) 32 μm particles, high voltage, and (h) 32 μm particles, low voltage.

accurate prediction of the collection efficiency than the ADE with lumped parameters.

COST ANALYSIS OF A WIRE-PLATE ESP

Main Costs Associated with a Wire-Plate ESP

Following Aa (1991), the cost evaluation problem was simplified analyzing the main costs in building and operating an ESP. The total cost is the combination of fixed construction costs and operation costs. The first are usually given by all internal parts, which are as follows:

1. cost of collecting plates, C_p [\$/m^2], including insulation and bottom guides;
2. cost of wire electrodes, C_f [\$/m^2], including insulation from external casing;
3. cost of casing, C_c [\$/m^2];
4. cost of high voltage power supply, C_t[\$], usually rectifier transformers;
5. cost of rapping mechanism, C_r[\$], including tumbling hammers;
6. cost of manpower needed to build the filter, C_m[\$].

Operational costs are mostly due to electric energy required (C_w[\$/kWh]) in a reference time period t. However, ESPs in service need maintenance to avoid wire breaking or internal corrosion, which could lead to a decrease in performance.

The total cost, C, to build and operate an ESP during the time period t may be expressed as follows:

$$C = C_w \cdot P \cdot t + C_f \cdot n_f + 2C_p \cdot L \cdot L_y + 2C_c \cdot L \cdot (L_y + h) + C_t + C_r + C_m, \qquad [10]$$

where P is the electric power to be supplied, n_f is the number of wires, and L, L_y, and h are length, height, and half-width of the precipitator, respectively. Detailed values of C_w, C_f, C_p, C_c, C_t, C_r, and C_m depend on local markets and are not easy to predict; however, in this article we assume the cost specimen proposed in Table 4.

Table 4
Cost specimen of a wire-plate ESP (*ABB Fläkt*)

External *casing*	\$ 17/m^2	C_c = \$ 20/m^2
Gas distribution screens	\$ 3/m^2	
Plate suspension system	\$ 5/m^2	C_p = \$ 28/m^2
Collecting plates	\$ 15/m^2	
Insulation system	\$ 8/m^2	
Wire suspension system	\$ 15/*wire*	C_f = \$ 34/*wire*
Emitting electrodes	\$ 9/*wire*	
Wire insulation system	\$ 10/*wire*	
Collector *rapping*		C_r = \$ 6,300
Electric equipment (rectifiers)		C_t = \$ 13,500 each
Manpower		C_m = \$ 71/h
Electric supply		C_w = \$ 0.25/kWh

Since in their basic configuration ESPs are energized by direct current, specific electric power ([kW/m^2]) may be derived by multiplying the potential applied to wires, V, by the current density, J, flowing to plates. This could be evaluated using the $\Delta V - J$ characteristic given by Cooperman (1981).

ESP Design Parameters

In the present model, according to Equation (10) and to the $\Delta V - J$ characteristic (Cooperman 1981), the parameters influencing the overall cost are as follows:

1. length of the precipitator, L;
2. electric potential applied to the wires, V;
3. wire-to-plate distance, h;
4. wire-to-wire distance, δ.

The cost of the rapping mechanism, C_r, of the transformer, C_t, and of the building manpower are almost fixed costs, having a slight dependence on the above-listed parameters. We may neglect their influence in the current analysis.

Since the specification to produce an ESP is the desired efficiency, η_d, given the process flow rate Q, optimizing an electrostatic precipitator consists of finding the optimal minimum to Equation (10). Thus we obtain the following equation:

$$\nabla C(V, L, h, \delta) = 0, \qquad [11]$$

where ∇ indicates the gradient operator, bound by the design efficiency, η_d:

$$\eta = \eta(V, L, h, \delta) = \eta_d. \qquad [12]$$

Since an exact relationship between C and the design parameters given the constraint on efficiency (12) is not straightforward, the analytical resolution of Equation (11) is not possible. It is, however, possible to evaluate the dependence of both efficiency and total cost of the precipitator on each of the design parameters we listed. The dependence of efficiency on design parameters will be evaluated using the ADE model fitted on DNS data presented previously.

RESULTS: INFLUENCE OF DESIGN PARAMETERS ON ESP COST

The potential use of the accurate two-dimensional, distributed parameters ADE model is demonstrated in the 2 case studies presented. The first considers a simple cost-analysis suitable for choosing from different possible alternatives for ESP revamping, which may be required to meet more stringent regulations. In the second, we consider a cost-effective design optimization problem focused on the identification of best design guidelines for ESP production.

Cost Sensitivity Analysis

To focus, consider a model ESP with the characteristics shown in Table 5. As observed before in Figure 4, according to our

Table 5
Base configuration of the wire-plate ESP considered

Precipitator length	$L = 0.4$ m
Wire-plate distance	$h = 0.02$ m
Distance between wires	$\delta = 0.0628$ m
Applied voltage	42 kV
Flow rate	21.63 m^3/h

model, the ESP model, which is 0.4 m long, has an efficiency of 87%. The objective of this section is to examine how any increase in efficiency depends on every single design parameter and how this required variation of each design parameter reflects on the overall cost of the ESP.

The present ADE model was used to calculate collection efficiency for different values of the electric potential, the wire-to-plate distance, the wire-to-wire distance, and the length of the ESP. We examined the influence of the variation of each single parameter, exploring a range of alternative values around the original configuration values, which are shown in Table 5. The wire-to-plate distance was changed in the range $0.002 \div 0.075$ m, the wire-to-wire distance in the range $0.03 \div 0.1$ m, the electric potential in the range $28 \div 57$ V, and the length of the ESP in the range $0. \div 0.8$ m.

Results show that the 4 μm particle collection efficiency increases when the electric potential and ESP length increase. Collection efficiency decreases when the wire-to-plate distance and the wire-to-wire distance increase.

For each configuration examined, the costs were also calculated to plot the cost-efficiency dependence shown in Figure 5. In this figure, each line corresponds to the set of simulations performed changing one single parameter (reported on the curve). The arrows indicate the direction in which the value of the single parameter increases. The point in common for all the curves is the pair efficiency cost corresponding to the reference configuration examined in Table 5.

If we consider the slope of the curves at their intersection, we will have information about the rate of cost increase necessary to improve the collection efficiency by varying each parameter. One remarkable result is that reducing the distance between wire electrodes, δ, improves ESP collection efficiency at the lowest cost: raising efficiency from 0.87 to 0.95 does not imply a significant increase of the total cost (<3%). To obtain the same efficiency increase by increasing the length of the ESP, L, or by increasing the electric potential, V, an increase in the total cost up to 23% and to 93% is entailed, respectively. Finally, Figure 5 shows that it would be extremely costly to improve even slightly the collection efficiency by increasing the wire-to-plate distance.

These considerations agree with the experimental results of Miller et al. (1998), obtained performing investigations on a laboratory scale wire-plate ESP. Pushed by these results, some suppliers are now considering the possibility of building precipitators with adjustable distance between wire electrodes (Grübbström 1999).

Economics of Wider Spacing ESP: Varying Both V *and* h

Since 1971, when the Japanese company Nippon Kay Heavy Co. first introduced wider spacing ESP, this design choice was endorsed by most ESP suppliers. The rationale is to reach the desired performances keeping as high as possible both duct width, $2h$, and applied voltage, V. The validity of the wide spacing approach was shown, among others, by Navarrete et al. (1997), who found experimentally that given the same specific corona currents, the collecting efficiencies of ESPs with wide spacing were higher than those with narrow spacing.

Starting from the reference configuration reported in Table 5, we allow both V and h to vary so that we can obtain the $\eta = \eta(V, h)$ and the $C = C(V, h)$ surfaces, which are shown in Figure 6. We considered values of V in the range $15 \div 85$ kV and values of h in the range $0.005 \div 0.105$ m. For each value of V and h, we calculated the electrostatic field, $\mathbf{E}(x, z)$, to determine the wall normal advection velocity (Equation (6)). The correct profile was calculated for the mean streamwise velocity, $u(x, z)$, considering that the flow rate does not change even with changes in the geometry of the ESP. Integrating Equation (4) gives $c(L, z)$ and then the value of η (Equation (5)) for the

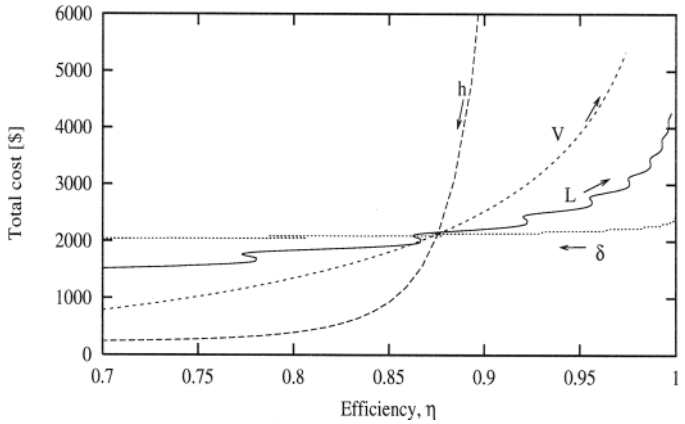

Figure 5. Sensitivity analysis of cost/efficiency function, $C = C(\eta)$, for the design parameters.

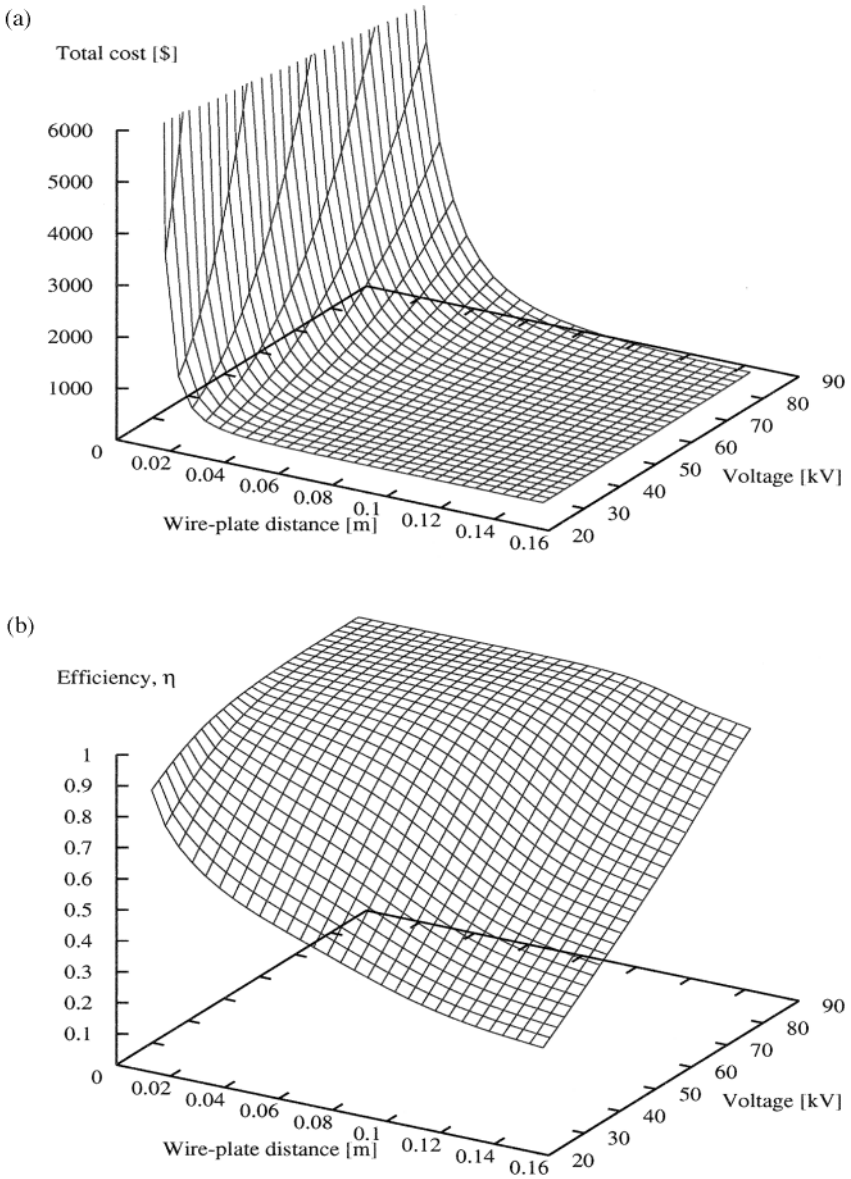

Figure 6. (a) Cost isosurface $C = C(V, h)$, and (b) efficiency isosurface $\eta = \eta(V, h)$.

chosen values of V and h. The same values of the parameters were used in Equation (10) to calculate the corresponding cost. This procedure was repeated for a sufficient number of (V, h) pairs and allowed to define the iso-efficiency and iso-cost surfaces shown in Figure 6.

As shown in the lower part of Figure 6, larger values of efficiency are associated with high voltage and reduced wire-plate distance. From the upper part of Figure 6, we observe that the surface representing the total cost is steeper in this region of the parameter space.

In real applications, collection efficiency is the constraint and the optimal solution is the one that allows us to achieve the desired efficiency minimizing the costs. A value for the collection efficiency ($\eta = 99\%$) was therefore fixed, i.e., we chose a fixed isocontour on the $\eta(h, V)$ surface, and we evaluated the cost of possible alternatives. Figure 7 shows the 99% isocontour of the collection efficiency surface in the plane corresponding to the parameter space. In this plane, each point that lies on the fixed efficiency isocontour is a possible alternative. These points correspond to different cost isocontours. In Figure 7, we show for reference 4 different cost isocontours. Values of (V, h) along the same cost isocontours identify specific ESP configurations having the same total cost. For each cost isocontour, only the pair (V, h) that also lies on the efficiency isocontour is a possible solution.

It is clear that the desired performance could be achieved with different values of applied voltage and duct width and that different costs are associated with each solution. As can be observed

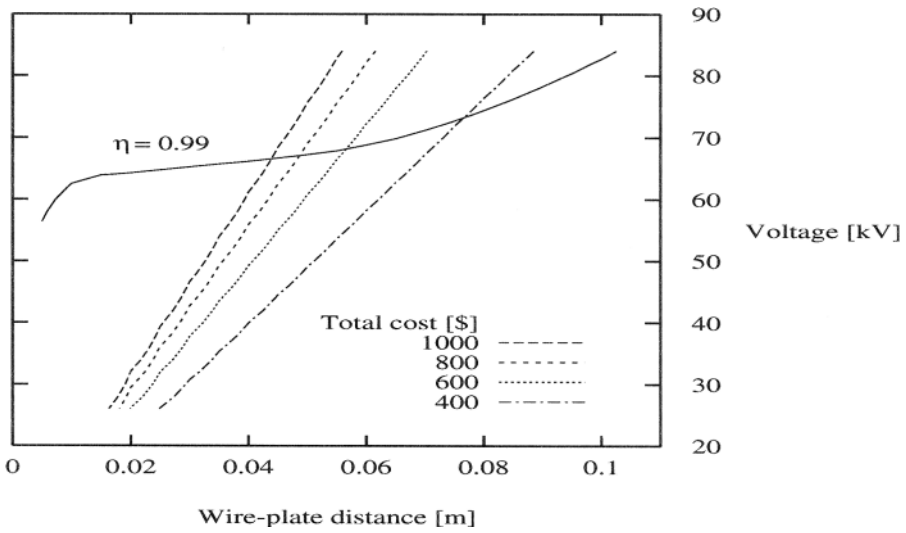

Figure 7. Intersection between efficiency isosurface $\eta = 0.99$ and different cost isosurfaces for wider space case analysis.

by the cost isocontour values, lower costs correspond to higher values of duct width. The global optimum, which is identified by the cost isocountour tangent to the fixed efficiency isocontour, is in the high potential and high wire-plate distance region of the parameter space. This proves that applying the wide spacing design leads to obtaining higher collection efficiencies with lower cost, as indicated by industrial practice.

CONCLUSIONS

New design methods of ESPs should be optimized in order to ensure meeting both the new environmental guidelines and the economics of the whole process. In other words, the highest efficiency at the lowest cost. We are carrying out a systematic research program on particle transport in ESPs in order to identify guidelines for optimal design (see also Cerbelli et al. 2001; Beux et al. 2002; Marchioli and Soldati 2002). Our investigation tool is the DNS of the flow field with Lagrangian tracking of particles. We were able to generate a database on which simpler design-oriented models, such as ADE models, can be tuned in order to perform complete investigations for a broader range of ESP design parameters. The objective of this paper was to devise an approach to perform the cost/efficiency analysis in a wire-plate ESP. Specifically, our aim was to examine the influence of ESP design parameters on particle transport and collection efficiency.

Through a simplified though rigorous cost analysis, we listed 4 design parameters that affect total costs: duct length and width and applied voltage and distance between the emitting electrodes. Since the cost/efficiency relationship, $C(\eta)$, may not be solved for directly, an ADE-based model was used with distributed parameters fitted on our DNS database and averaged quantities in order to calculate the efficiency for each given set of design parameters. Then the cost associated with the same set of design parameters was calculated, obtaining the relationship between the efficiency and the cost that allows us to find the optimal design set.

A first result indicates that reducing the distance between wires allows for improved efficiency at the lowest cost. This is due to an increase in the mean electric field and to a significant reduction in the current per wire flowing to plates. This result confirms on a theoretical basis the previous observations by Miller et al. (1998) based on experimental investigations.

Our results also show that the wider spacing design is cost effective. Wider spacing achieves the performance desired at lower costs, because first, increasing the duct width leads to a reduction in the flowing current, and therefore in the electric power consumption, and second, the higher voltage ensures a mean electric field high enough to collect particles.

REFERENCES

Aa, P. (1991). Reviving an Electrostatic Precipitator, *Chem. Eng*. 11:217–222.

Beux, F., Iollo, A., Salvetti, M. V., and Soldati, A. (2001). Approximation and Reconstruction of the Electrostatic Field in Wire-Plate Precipitators by a Low-Order Model, *J. Comp. Phys*. 170:893–916.

Beux, F., Iollo, A., Salvetti, M. V., and Soldati, A. (2002). Current-Density Approximation for Efficient Computation of the Electrostatic Field in Wire-Plate Precipitators, *IEEE Trans. Ind. Appl*. 38:858–865.

Cerbelli, S., Giusti, A., and Soldati, A. (2001). ADE Approach to Predicting Particle Dispersion in Wall Bounded Turbulent Flows, *Int. J. Multiphase Flow* 27:1861–1879.

Choi, B. S., and Fletcher, C. A. J. (1997). Computation of Particle Transport in an Electrostatic Precipitator, *J. Electrostatics* 40&41:413–418.

Choi, B. S., and Fletcher, C. A. J. (1998). Turbulent Particle Dispersion in an Electrostatic Precipitator, *Appl. Math. Modell*. 22:1009–1021.

Cooperman, G. (1981). New Current-Voltage Relation for Duct Precipitators Valid for Low and High Current Densities, *IEEE Trans. Ind. Appl*. 17:236–239.

Deutsch, W. (1922). Bewegung und ladung der elektricitatstrager in zylinder kondensator, *Ann. Phys*. 58:335–343.

Egli, W., Kogelschatz, U., Gerteisen, E. A., and Gruber, R. (1997). 3D Computation of Corona, Ion Induced Secondary Flows and Particle Motion in Technical ESP Configurations, *J. Electrostatics* 40&41:425–430.

Gallimberti, I. (1998). Recent Advancements in the Physical Modelling of Electrostatic Precipitators, *J. Electrostatics* 43:219–247.

Grübbström, J. (1999). *Private communication*, Udine.

Kallio, G. A., and Stock, D. E. (1992). Interaction of Electrostatic and Fluid Dynamic Fields in Wire-Plate Electrostatic Precipitators, *J. Fluid Mech*. 240:133–154.

Kihm, K. D. (1987). *Effects of Nonuniformities on Particle Transport in Electrostatic Precipitators*, Ph.D. dissertation, Department of Mechanical Engineering, Stanford University, Stanford, CA.

Kihm, K. D., Mitchner, M., and Self, S. A. (1985). Comparison of Wire-Plate and Plate-Plate Electrostatic Precipitators in Laminar Flow, *J. Electrostatics* 17:193–208.

Kim, S. K., and Lee, K. W. (1999). Experimental Study of Electrostatic Precipitators and Comparison with Existing Theoretical Prediction Models, *J. Electrostatics* 48:3–25.

Ko, J.-H., and Ihm, S.-K. (1997). A Two-Dimensional Model for Polydisperse Particles on the Effective Migration Rate of the Electrostatic Precipitator with Wider Spacing, *Aerosol Sci. Technol*. 26:398–402.

Kontomaris, K., and Hanratty, T. J. (1994). Effect of Molecular Diffusivity on Point Source Diffusion in the Centre of a Numerically Simulated Turbulent Channel Flow, *Int. J. Heat and Mass Transfer* 37:1817–1826.

Larsen, P. S., and Sørensen, S. K. (1984). Effect of Secondary Flows and Turbulence on Electrostatic Precipitator Efficiency, *Atmos. Environ*. 18:1964–1967.

Leonard, G. L., Mitchner, M., and Self, S. A. (1980). Particle Transport in Electrostatic Precipitators, *Atmos. Environ*. 14:1289–1299.

Leutert, G., and Bohlen, B. (1972). The Spatial Trend of Electric Field Strength and Space Charge Density in Plate Type Electrostatic Precipitator, *Staub Reinhalt Luft* 32:27–40 (in English).

Marchioli, C., and Soldati, A. (2002). Mechanisms for Particle Transfer and Segregation in Turbulent Boundary Layer, *J. Fluid Mech*. 468:283–315.

Miller, J., Hoferer, B., and Schwab, A. J. (1998). The Impact of Corona Electrode Configuration on Electrostatic Precipitator Performance, *J. Electrostatics* 44:67–75.

Moin, P., and Mahesh, K. (1998). Direct Numerical Simulation: A Tool in Turbulence, *Ann. Rev. Fluid Mech*. 30:539–578.

Monticelli, E. (1999). *Particle Transport Characterization for Optimal Design of Electrostatic Precipitators*, M.S. thesis, University of Udine, Italy (in Italian).

Navarrete, B., Cañadas, L., Cortes, V., Salvador, L., and Galindo, J. (1997). Influence of Plate Spacing and Ash Resistivity on the Efficiency of Electrostatic Precipitators, *J. Electrostatics* 39:65–81.

Self, S. A., Mitchner, M., and Kihm, K. D. (1987). Precipitator Performance Improvement through Turbulence Control, *Proc. Int. Conf. on Electrostatic Precipitators*, Avano/Venice, Italy, pp. 443–481.

Sisti, C. A. (1997). *Lagrangian Simulation of Turbulent Aerosol Dispersion in Electrostatic Precipitators*, M.S. thesis, University of Udine, Italy (in Italian).

Soldati, A. (2000). On the Effects of ElectroHydroDynamic Flows and Turbulence on Aerosol Transport and Collection in Wire-Plate Electrostatic Precipitators, *J. Aerosol Sci*. 31:293–305.

Soldati, A. (2002). Influence of Large-Scale Streamwise Vortical EHD Flows on Wall Turbulence, *Int. J. Heat Fluid Flow* 23:441–443.

Soldati, A., Andreussi, P., and Banerjee, S. (1993). Direct Numerical Simulation of Turbulent Particle Transport in Electrostatic Precipitators, *AIChE J*. 39:1910–1919.

Soldati, A., Andreussi, P., and Banerjee, S. (1995). Direct Numerical Simulation of Turbulent Particle Transport in Electrostatic Precipitators—Reply, *AIChE J*. 41:739–740.

Soldati, A., and Banerjee, S. (1998). Turbulence Modification by Large-Scale Organized Electrohydro-Dynamic Flows, *Phys. Fluids* 10:1742–1756.

Soldati, A., Casal, M., Andreussi, P., and Banerjee, S. (1997). Lagrangian Simulation of Turbulent Particle Dispersion in Electrostatic Precipitators, *AIChE J*. 43:1403–1413.

Soldati, A., and Marchioli, C. (2001). Prospects for Modulation of Turbulent Boundary Layer by EHD Flows. In *Turbulence Structure and Modulation*, edited by A. Soldati and R. Monti. Springer Verlag, New York, pp. 119–160.

Taylor, G. I. (1921). Diffusion by Continuous Movements, *Proc. Lond. Math. Soc*. 20:196–204.

Tennekes, H., and Lumley, J. L. (1976). *A First Course in Turbulence*, MIT Press, Cambridge, Massachussetts.

Williams, J. C., and Jackson, R. (1962). The Motion of Solid Particles in an Electrostatic Precipitator, *Proc. Symp. Trans. Inst. Chem. Engrs*. 282–288.

Yamamoto, T., and Velkoff, H. R. (1981). Electrohydrodynamics in an Electrostatic Precipitator, *J. Fluid Mech*. 108:1–15.

Zhuang, Y., Kim, Y. J., Lee, T. G., and Biswas, P. (2000). Experimental and Theoretical Studies of Ultra-Fine Particle Behavior in Electrostatic Precipitators, *J. Electrostatics* 48:245–260.